

Re-evaluation of SNP heritability in complex human traits

Doug Speed,^{1,□} Na Cai,^{2,3} the UCLEB Consortium,⁴ Michael R. Johnson,⁵ Sergey Nejentsev,⁶ David J Balding.^{1,7}

¹ UCL Genetics Institute, University College London, United Kingdom.

² Wellcome Trust Sanger Institute, Wellcome Genome Campus, Hinxton, Cambridge, United Kingdom.

³ European Molecular Biology Laboratory, European Bioinformatics Institute (EMBL-EBI), Wellcome Genome Campus, Hinxton, Cambridge, United Kingdom.

⁴ A full list of members and affiliations appears in the Supplementary Material.

⁵ Division of Brain Science, Imperial College London, United Kingdom.

⁶ Department of Medicine, University of Cambridge, United Kingdom.

⁷ Centre for Systems Genomics, School of BioSciences and School of Mathematics & Statistics, University of Melbourne, Australia.

□Corresponding author: doug.speed@ucl.ac.uk

Abstract

SNP heritability, the proportion of phenotypic variance explained by SNPs, has been reported for many hundreds of traits. Its estimation requires strong prior assumptions about the distribution of heritability across the genome, but the assumptions in current use have not been thoroughly tested. By analyzing imputed data for a large number of human traits, we empirically derive a model that more accurately describes how heritability varies with minor allele frequency, linkage disequilibrium and genotype certainty. Across 19 traits, our improved model leads to estimates of common SNP heritability on average 43% (standard deviation 3) higher than those obtained from the widely-used software GCTA, and 25% (standard deviation 2) higher than those from the recently-proposed extension GCTA-LDMS. Previously, DNaseI hypersensitivity sites were reported to explain 79% of SNP heritability; using our improved heritability model their estimated contribution is only 24%.

Introduction

The SNP heritability (h^2_{SNP}) of a trait is the fraction of phenotypic variance explained by additive contributions from SNPs.¹ Accurate estimates of h^2_{SNP} are central to resolving the missing heritability debate, indicate the potential utility of SNP-based prediction and help design future genome-wide association studies (GWAS).^{2,3} Whereas techniques for estimating (total) heritability have existed for decades,^{4,5} the first method for estimating h^2_{SNP} was proposed only in 2010,¹ but has since been applied to many hundreds of traits. Extensions of this method are now being used to partition heritability across chromosomes, biological pathways and by SNP function, and to calculate the genetic correlation between pairs of traits.⁶⁻⁸

As the number of SNPs in a GWAS is usually much larger than the number of individuals, estimation of h^2_{SNP} requires steps to avoid over-fitting. Most reported estimates of h^2_{SNP} are based on assigning the same Gaussian prior distribution to each SNP effect size, in a way which implies that all SNPs are expected to contribute equal heritability.^{1,9} By examining a large collection of real datasets, we derive approximate relationships between the expected heritability of a SNP and minor allele frequency (MAF), levels of linkage disequilibrium (LD) with other SNPs and genotype certainty. This provides us with an improved model for heritability estimation and a better understanding of the genetic architecture of complex traits.

Results

When estimating h^2_{SNP} , the “LDAK Model” assumes

$$E[h_j^2] \sim [f_j(1-f_j)]^{1+\alpha} \times w_j \times r_j, \quad (1)$$

where $E[h_j^2]$ is the expected heritability contribution of SNP j and f_j is its (observed) MAF. The parameter α determines the assumed relationship between heritability and MAF. In human genetics it is commonly assumed that heritability does not depend on MAF, which is achieved by setting $\alpha=1$, however, we consider alternative relationships. The SNP weights w_1, \dots, w_m are computed based on local levels of LD;⁹ w_j tends to be higher for SNPs in regions of low LD, and thus the LDAK Model assumes that these SNPs contribute more than those in high-LD regions. Finally, $r_j \in [0,1]$ is an information score measuring genotype certainty; the LDAK Model expects that higher-quality SNPs contribute more than lower-quality ones. r_j is defined in Online Methods, where we also explain how (1) arises by assuming a genome-wide random regression in which SNP effect sizes are assigned Gaussian distributions.

62 The “GCTA Model” is obtained from (1) by setting $w_j=1$ and $r_j=1$, and thus assumes that expected heritability does not
63 vary with either LD or genotype certainty. To date, most reported estimates of h^2_{SNP} have used the GCTA Model with
64 $\alpha=-1$, which corresponds to the assumption that $E[h^2_j]$ is constant, and so the expected contribution of a SNP set
65 depends only on the number of SNPs it contains.¹ To appreciate the major difference between the GCTA and LDK
66 Models, consider a region containing two SNPs: under the GCTA Model, the expected heritability of these two SNPs is
67 the same irrespective of the LD between them, whereas under the LDK Model, two SNPs in perfect LD are expected
68 to contribute only half the heritability of two SNPs showing no LD. See Figure 1 for a more detailed example.

70 **FIGURE 1 ABOUT HERE**

71
72 An alternative method for estimating h^2_{SNP} is LDSC (LD Score Regression).¹⁰ The LDSC Model expects that each SNP
73 contributes equal heritability,^{10,11} and therefore closely resembles the GCTA Model with $\alpha=-1$. When applied to the
74 same dataset, estimates from LDSC will typically have standard error 25-100% higher than those from GCTA;¹¹ this is
75 partly because the LDSC Model includes an extra parameter, designed to capture confounding biases, and partly
76 because LDSC estimates are moment-based, whereas GCTA (like LDK) uses restricted maximum likelihood
77 (REML).^{12,13} However, as LDSC requires only summary statistics (i.e., p-values from single-SNP analysis), it can be
78 used on much larger datasets than GCTA and LDK, which need raw genotype data, and can be applied to results from
79 large-scale meta-analyses.¹⁰

80
81 **SNP partitioning:** (1) can be generalized by dividing SNPs into tranches across which the constant of proportionality is
82 allowed to vary (so $E[h^2_j]=c_k \times [f_j(1-f_j)]^{1+\alpha} \times w_j \times r_j$ for SNPs in Tranche k). This is known as SNP partitioning.⁶ Two
83 examples are GCTA-MS¹⁴ and GCTA-LDMS.¹⁵ when applied to common SNPs (MAF>0.01), GCTA-MS divides the
84 genome into five tranches based on MAF, using the boundaries 0.1, 0.2, 0.3 and 0.4, while GCTA-LDMS first divides
85 SNPs into four tranches based on local average LD Score,¹⁰ then divides each of these into five based on MAF, resulting
86 in a total of 20 tranches. In general, we prefer to avoid SNP partitioning when estimating h^2_{SNP} , because it introduces
87 (often arbitrary) discontinuities in the model assumptions and can cause convergence problems. However, we show
88 below that partitioning based on MAF enables reliable estimation of h^2_{SNP} when rare SNPs (MAF<0.01) are included.
89 Additionally, SNP partitioning provides a way to visually assess the fit of different heritability models; it allows us to
90 estimate average h^2_j for different SNP tranches, which can then be compared to the values predicted under different
91 assumptions.

93 **TABLE 1 ABOUT HERE**

94
95 **Datasets:** In total, we analyze data for 42 traits. Table 1 describes the 19 "GWAS traits" (17 case-control, 2
96 quantitative). For these, individuals were genotyped using either genome-wide Illumina or Affymetrix arrays (typically
97 500K to 1.2M SNPs). We additionally examine data from eight cohorts of the UCLEB consortium,²⁴ which comprise
98 about 14000 individuals genotyped using the Metachip,²⁵ (a relatively sparse array of 200K SNPs selected based on
99 previous GWAS) and recorded for a wide range of clinical phenotypes. From these, we consider 23 quantitative
100 phenotypes (average sample size 8200), which can loosely be divided into anthropomorphic (height, weight, BMI and
101 waist circumference), physiological (lung capacity and blood pressure), cardiac (e.g., PR and QT intervals), metabolic
102 (glucose, insulin and lipid levels) and blood chemistry (e.g., fibrinogen, Interleukin 6 and haemoglobin levels). In
103 general, our quality control is extremely strict; after imputation we retain only autosomal SNPs with MAF>0.01 and
104 information score $r_j>0.99$. We only relax quality control when, using the UCLEB data, we explicitly examine the
105 consequences of including lower-quality and rare SNPs.

106
107 Further details of our methods and datasets are provided in Online Methods. In particular, we explain how when
108 estimating h^2_{SNP} we give special consideration to highly-associated SNPs, which we define as those with

109 $P < 10^{-20}$ from single-SNP analysis, and how for the UCLEB data, we confirm that genotyping errors do not correlate
110 with phenotype (which is important for the analyses where we include lower-quality SNPs).

111
112 **Relationship between heritability and MAF:** Varying the value of α in (1) changes the assumed relationship between
113 heritability and MAF; three example relationships are shown in Figure 2a. To determine suitable α , we analyze each of
114 the 42 traits using seven values: -1.25, -1, -0.75, -0.5, -0.25, 0 and 0.25, seeing which lead to best model fit (highest
115 likelihood). Full results are provided in Supplementary Figure 1 and Supplementary Table 2. First, to remove any
116 confounding due to LD, we use only a pruned subset of SNPs (with $w_j=1$); next, we repeat without LD pruning (the
117 results for the GWAS traits are shown in Figure 2b); finally, for the UCLEB traits, we repeat including lower-quality
118 and rare SNPs. We find that model fit is typically highest for $-0.5 \leq \alpha \leq 0$, whereas the most widely-used value, $\alpha=-1$,
119 results in sub-optimal fit. On the basis that it performs consistently well across different traits and SNP filterings, we
120 recommend that $\alpha=-0.25$ becomes the default. This value implies that expected heritability declines with MAF; this is
121 seen in Figure 2a which reports, averaged across the 19 GWAS traits, the (weight-adjusted) per-SNP heritability for
122 low- and high-MAF SNPs (see Supplementary Figure 2 for further details).

123

124 **FIGURE 2 ABOUT HERE**

125
126 While $\alpha=-0.25$ provides the best fit overall, for individual traits, optimal α may differ, and therefore we investigate
127 sensitivity of h^2_{SNP} estimates to the value of α . Full results are provided in Supplementary Figures 3, 4 & 5, while Figure
128 6a provides a summary for the UCLEB traits. When analyzing only common SNPs, we find that changes in α have little
129 impact on h^2_{SNP} . For example, across the 23 UCLEB traits, estimates from high-quality common SNPs using $\alpha=-0.25$
130 are on average only 5% (standard deviation 4) lower than those using $\alpha=-1$, and 4% (standard deviation 4) higher than
131 those using $\alpha=0$. However, this is no longer the case when rare SNPs are included in the analysis: for example, when the
132 MAF threshold is reduced to 0.0005, estimates using $\alpha=-0.25$ are on average 18% (standard deviation 4) lower than
133 those using $\alpha=-1$ and 30% (standard deviation 6) higher than those from $\alpha=0$. Therefore, when including rare SNPs, we
134 guard against misspecification of α by partitioning based on MAF (with boundaries at 0.001, 0.0025, 0.01 and 0.1); we
135 find that this provides stable estimates of h^2_{SNP} and also allows estimation of the relative contributions of rare and
136 common variants (Figure 6a and Supplementary Figure 6).

137
138 **Relationship between heritability and LD:** The LDAK Model assumes that heritability varies according to local
139 levels of LD, whereas the GCTA Model assumes that heritability is independent of LD. First we demonstrate that
140 choice of model matters when estimating h^2_{SNP} . For the GWAS traits, Figure 3a reports relative estimates of h^2_{SNP} from
141 GCTA, GCTA-MS, GCTA-LDMS and LDAK (all using $\alpha=-0.25$); see Supplementary Figure 7 for an extended version.
142 We find that estimates based on the LDAK Model are on average 48% (standard deviation 3) higher than estimates
143 based on the GCTA Model. For the UCLEB traits, estimates from LDAK are on average 88% (standard deviation 7)
144 higher than those from GCTA (Supplementary Fig. 8). Figure 3a also includes results from LDSC, run as described in
145 the original publication¹⁰ (see Supplementary Table 3 for numerical values). Estimates from LDSC are not significantly
146 different to those from GCTA, which is to be expected considering that GCTA and LDSC assume the same relationship
147 between heritability and LD. In Supplementary Figure 9 we consider alternative versions of LDSC (e.g., varying how
148 LD Scores are computed, forcing the intercept term to be zero and excluding highly-associated SNPs). While changing
149 settings can have a large impact, in all cases the average estimate of h^2_{SNP} from LDSC remains substantially below that
150 from LDAK.

151
152 **FIGURE 3 ABOUT HERE**

153
154 A recent article which asserted that GCTA estimates h^2_{SNP} more accurately than LDAK, based this claim on a simulation
155 study in which causal SNPs were assigned effect sizes from the same Gaussian distribution, irrespective of LD.⁶ This
156 resembles the GCTA Model but not the LDAK Model, and so it is no surprise that GCTA performed better. Figure 3b
157 shows that if instead effect size variances had been scaled by SNP weights, and so vary with LD similar to the LDAK
158 Model, then the study would have found LDAK to be superior to GCTA. Thus using simulations to compare different
159 heritability models is problematic, because the conclusions will depend on the assumptions used when generating
160 phenotypes. See Supplementary Figure 10 for a full reanalysis of the reported simulation study and Supplementary
161 Figure 11 for further simulations.

162
163 Rather than using simulations, we compare LDAK and GCTA empirically. Supplementary Table 4 shows that when $\alpha=-$
164 0.25, assuming the LDAK Model leads to higher likelihood than assuming the GCTA Model for all 19 GWAS traits and
165 for 17 of the 23 UCLEB traits (if we instead use $\alpha=-1$, likelihood is higher under the LDAK Model for 31 of the 42
166 traits). To visually demonstrate the superior fit of the LDAK Model, we partition SNPs into low- and high-LD tranches
167 (for this, we rank SNPs according to the average LD Score¹⁰ of non-overlapping 100kb segments, the metric used by
168 GCTA-LDMS¹⁵). First, we partition so that the two tranches contain an equal number of SNPs. The left half of Figure 4
169 reports, for each of the GWAS traits, the contribution of the low-LD tranche, estimated using the GCTA Model (with
170 $\alpha=-0.25$). Under the GCTA Model, the low-LD tranche is expected to contribute 50% of h^2_{SNP} ; under the LDAK Model,
171 it is expected to contribute 72% of h^2_{SNP} . We see that the estimated contribution of the low-LD tranche is consistent with
172 the GCTA Model (95% confidence interval includes 50%) for only 5 of the 19 traits, whereas it is consistent with the
173 LDAK Model (confidence interval includes 72%) for 18. Next we partition so that the low-LD tranche contains a
174 quarter of the SNPs; now the low-LD tranche is predicted to contribute 26% of h^2_{SNP} under the GCTA Model, but 47%
175 of h^2_{SNP} under the LDAK Model. The right half of Figure 4 shows that its estimated contribution is consistent with the
176 GCTA Model for only 7 of the 19 traits, but again consistent with the LDAK Model for 18. Additional results are
177 provided in Supplementary Figure 12; these show that regardless of whether we estimate heritabilities using LDAK
178 (rather than GCTA), whether we use $\alpha=-1$ (instead of $\alpha=-0.25$) or whether we analyze the UCLEB traits, it remains the
179 case that the LDAK Model better predicts the heritability contribution of each tranche than the GCTA Model.

180
181 **FIGURE 4 ABOUT HERE**

182
183 **Relationship between heritability and genotype certainty:** The LDAK Model assumes that SNP heritability
184 contributions vary with genotype certainty (measured by the information score r_j). So far, our analyses have used only
185 very high-quality SNPs ($r_j>0.99$), so this assumption has been redundant. Now we also include lower-quality common
186 SNPs; we focus on the UCLEB traits, as for these we were able to test for correlation between genotyping errors and

187 phenotype (Supplementary Fig. 13). Supplementary Table 5 compares model fit with and without allowance for
188 genotype certainty; it shows that including r_j in the heritability model tends to provide a modest improvement in model
189 fit, resulting in a higher likelihood for 18 out of 23 traits.
190

191 **Estimates of h^2_{SNP} for the GWAS traits:** Table 1 presents our final estimates of h^2_{SNP} for the 19 GWAS traits, obtained
192 using the LDAK Model (with $\alpha=-0.25$). For comparison, we include previously-reported estimates of h^2_{SNP} , as well as
193 the proportion of phenotypic variance explained by SNPs reported as genome-wide significant (see Supplementary
194 Table 6). For the disease traits, estimates are on the liability scale, obtained by scaling according to the observed case-
195 control ratio and (assumed) trait prevalence.^{26,27} We are unable to find previous estimates of h^2_{SNP} for tuberculosis or
196 intraocular pressure, indicating that for these two traits, we are the first to establish that common SNPs contribute
197 sizable heritability. Extended results are provided in Supplementary Table 7. These show that our final estimates of
198 h^2_{SNP} are on average 43% (standard deviation 3) and 25% (standard deviation 2) higher than, respectively, those
199 obtained using the original versions (i.e., with $\alpha=-1$) of GCTA²⁸ and GCTA-LDMS.¹⁵ Results for the UCLEB Traits are
200 provided in Supplementary Table 1.
201

202 **Role of DNaseI hypersensitivity sites (DHS):** Gusev *et al.*⁷ used SNP partitioning to assess the contributions of
203 SNP classes defined by functional annotations. Across 11 diseases they concluded that the majority of h^2_{SNP} was
204 explained by DHS, despite these containing less than 20% of all SNPs. For Figure 5, we perform a similar analysis
205 using the 10 traits we have in common with their study (for 9 of these, we are using the same data). When we copy
206 Gusev *et al.* and assume the GCTA Model with $\alpha=-1$, we estimate that on average DHS contribute 86% (standard
207 deviation 4) of h^2_{SNP} , close to the value they reported (79%). When instead we assume the LDAK Model (with $\alpha=-$
208 0.25), the estimated contribution of DHS reduces to 25% (standard deviation 2). Under the LDAK Model, DHS are
209 predicted to contribute 18% of h^2_{SNP} so 25% represents 1.4-fold enrichment. To add context, we also consider "genic"
210 SNPs, which we define as SNPs inside or within 2kb of an exon (using RefSeq annotations²⁹), and "inter-genic," SNPs
211 further than 125kb from an exon; these definitions ensure that these two SNP classes are also predicted to contribute
212 18% of h^2_{SNP} under the LDAK Model. We estimate that genic SNPs contribute 29% (standard deviation 2), while inter-
213 genic SNPs contribute 10% (standard deviation 2), representing 1.6-fold and 0.6-fold enrichment, respectively. When
214 we extend this analysis to all 42 traits, DHS on average contribute 24% (standard deviation 2) of h^2_{SNP} , and in contrast
215 to Gusev *et al.*, enrichment remains constant when we reduce SNP density (Supplementary Fig. 14 & 15 and
216 Supplementary Table 8).
217

218 Finucane *et al.*³⁰ performed a similar analysis, but considered 52 SNP classes and estimated enrichment using LDSC;
219 across nine traits, they identified five classes with >4-fold enrichment, the highest of which, "conserved SNPs," had 13-
220 fold enrichment. When we use LDAK to estimate enrichment for our 19 GWAS traits, the results are more modest; the
221 highest enrichment is 2.5-fold, with only 1.3-fold enrichment for conserved SNPs (Supplementary Fig. 16).
222

223 FIGURE 5 ABOUT HERE

224
225 **Relaxing quality control:** For the UCLEB data, we consider nine alternative SNP filterings. Supplementary Figure 17
226 reports estimates of h^2_{SNP} for each trait / filtering, while Figure 6a provides a summary. First we vary the information
227 score threshold: $r_j > 0.99$, > 0.95 , > 0.9 , > 0.6 , > 0.3 and > 0 (each time continuing to require $\text{MAF} > 0.01$). Simulations
228 suggest that by including all 8.8M common SNPs ($r_j > 0$), instead of using just the 353K high-quality ones ($r_j > 0.99$), we
229 can expect estimates of h^2_{SNP} to increase by 50-60% (Supplementary Fig. 18). This is similar to what we observe in
230 practice, as across the 23 traits, estimates of h^2_{SNP} (using $\alpha=-0.25$) are on average 45% (standard deviation 8) higher.
231 The simulations further predict that, even though the Metabochip provides relatively low coverage of the genome (after
232 quality control, it contains only 60K SNPs, predominately within genes), we can expect estimates of h^2_{SNP} to be
233 approximately 80% as high as those obtained starting from genome-wide genotyping arrays. While we are unable to test
234 this claim directly, it is consistent with our results for height, body mass index and QT Interval, the three traits for which
235 reasonably precise estimates of common SNP h^2_{SNP} are available⁶ (Figure 6b). For the final three SNP filterings, we
236 vary the MAF threshold: $\text{MAF} > 0.0025$, $\text{MAF} > 0.001$ and $\text{MAF} > 0.0005$ (all with $r_j > 0$). Across the 23 traits, we find that
237 rare SNPs contribute substantially to h^2_{SNP} : for example, when we use the 17.3M SNPs with $\text{MAF} > 0.0005$, estimates of
238 h^2_{SNP} (using $\alpha=-0.25$ and MAF partitioning) are on average 29% (standard deviation 12) higher than those based on the
239 8.8M common SNPs (median increase 22%), with rare SNPs contributing on average 33% (standard deviation 5) of
240 h^2_{SNP} (Figure 6a).
241

242 FIGURE 6 ABOUT HERE

243 Discussion

244
245
246 With estimates of h^2_{SNP} so widely reported, it is easy to forget that calculating the variance explained by large numbers
247 of SNPs is a challenging problem. To avoid over-fitting, it is necessary to make strong prior assumptions about SNP
248 effect sizes, but different assumptions can lead to substantially different estimates of h^2_{SNP} . Previous attempts to assess
249 the validity of assumptions have used simulation studies,^{14,15} but this approach will tend to favor assumptions similar to

250 those used to generate the phenotypes. Instead, we have compared different heritability models empirically, by
251 examining how well they fit real datasets.

252
253 We begun by investigating the relationship between heritability and MAF. Across 42 traits, we found that best fit was
254 achieved by setting $\alpha=-0.25$ in (1), which implies that average heritability varies with $[\text{MAF}(1-\text{MAF})]^{0.75}$. As explained
255 in Online Methods, the value of α corresponds to the scaling of genotypes. Therefore, our result indicates that the
256 performance (i.e., detection power and/or prediction accuracy) of many penalized and Bayesian regression methods, for
257 example, the Lasso, ridge regression and BayesA,^{31,32} could be improved simply by changing how genotypes are scaled.
258 Although we recommend $\alpha=-0.25$ as the default value, with sufficient data available, it should be possible to estimate α
259 on a trait-by-trait basis, or to investigate more complex relationships between heritability and MAF. In particular, with a
260 better understanding of the relationship between heritability and MAF for low frequencies, it may no longer be
261 necessary to partition by MAF when rare SNPs are included.

262
263 We also examined the relationship between heritability and LD. To date, most estimates of h^2_{SNP} have been based on the
264 GCTA Model; this model can be motivated by a belief that each SNP is expected to have the same effect on the
265 phenotype, from which it follows that the expected heritability of a region should depend on the number of SNPs it
266 contains. By contrast, the LDAK Model views highly-correlated SNPs as tagging the same underlying variant, and
267 therefore believes that the expected heritability of a region should vary according to the total amount of distinct genetic
268 variation it contains. Across our traits, we found that the relationship between heritability and LD specified by the
269 LDAK Model consistently provides a better description of reality.

270
271 This finding has important consequences for complex trait genetics. Firstly, it implies that for many traits, common
272 SNPs explain considerably more phenotypic variance than previously reported, which represents a significant advance
273 in the search for missing heritability.² It also impacts on a large number of closely-related methods. For example,
274 LDSC,¹⁰ like GCTA, assumes that heritability contributions are independent of LD and therefore it also tends to under-
275 estimate h^2_{SNP} . Similarly, we have shown that estimates of the relative importance of SNP classes via SNP partitioning
276 can be misleading when the GCTA Model is assumed.^{7,30} Further afield, most software for mixed model association
277 analyses (e.g., FAST-LMM, GEMMA, MLM-LOCO and BOLT) use an extension of the GCTA Model,³³⁻³⁶ and
278 likewise most bivariate analyses, including those performed by LDSC.^{8,37,38} It remains to be seen how much these
279 methods would be affected if they employed more realistic heritability models.

280
281 Attempts have been made to improve the accuracy of heritability models via SNP partitioning.^{14,15,39} We find that
282 partitioning by MAF can be advantageous, as it guards against misspecification of the relationship between heritability
283 and MAF when rare variants are included. Figure 3a and Supplementary Figure 7 indicate that the realism of the GCTA
284 Model can be improved by partitioning based on LD; for example, across the GWAS traits, estimates from GCTA-
285 LDMS are on average 16% (standard deviation 2) higher than those from GCTA, and now only 23% (standard deviation
286 2) lower than those from LDAK. The improvement arises because model misspecification is reduced by allowing SNPs
287 in lower-LD tranches to have higher average heritability. However, Supplementary Table 9 illustrates why we consider
288 such an approach sub-optimal; in particular, SNP partitioning can be computationally expensive, and even with LD-
289 partitioning, model fit tends to be worse than that from LDAK.

290
291 While we have investigated the role of MAF, LD and genotype certainty, there remain other factors on which
292 heritability could depend, in particular the available functional annotations of genomes.⁴⁰ For example, our comparison
293 of genic and inter-genic SNPs indicates that the effect-size prior distribution could be improved by taking into account
294 proximity to coding regions. By way of demonstration, Supplementary Table 10 shows that model fit is improved by

$$E[h_j^2] = c_k \times [f_j(1-f_j)]^{1+\alpha} \times w_j \times r_j \times \exp\left(\frac{-(D_j+50)}{500}\right)$$

295 assuming , where D_j is the distance (in kb) between SNP
296 j and the nearest exon (under this model, genic SNPs are expected to have about twice the heritability of inter-genic
297 SNPs). In general, we believe that modifications of this type will have a relatively small impact; we note that across the

298 19 GWAS traits, scaling by $\exp\left(\frac{-(D_j+50)}{500}\right)$ increases model log likelihood by on average only 1.5, much less than
299 the average increase obtained by using $\alpha=-0.25$ instead of $\alpha=-1$ (8.9), or by choosing the LD-model specified by LDAK
300 instead of GCTA (17.7), and does not significantly change estimates of h^2_{SNP} . However, with sufficient data, it may be
301 possible to obtain more substantial improvement by tailoring model assumptions to individual traits.

302
303 When estimating h^2_{SNP} , care should be taken to avoid possible sources of confounding. Previously, we advocated a test
304 for inflation of h^2_{SNP} due to population structure and familial relatedness.³ The conclusions of a recent paper claiming
305 that h^2_{SNP} estimates are unreliable,⁴¹ would have changed substantially had this test been applied (Supplementary Fig.
306 19). We also recommend testing for inflation due to genotyping errors, particularly before including lower-quality
307 and/or rare SNPs. For the 23 UCLEB traits, we showed that including poorly-imputed SNPs resulted in significantly

308 higher estimates of h^2_{SNP} and made it possible to capture the majority of genome-wide heritability despite the very
309 sparse genotyping provided by the Metachip. We found that including rare SNPs also led to significantly higher h^2_{SNP} .
310 Although sample size prevented us from obtaining precise estimates of h^2_{SNP} for individual traits, our analyses indicated
311 that for larger datasets, including rare SNPs will be both practical and fruitful in the search for the remaining missing
312 heritability.²

313 314 **URLs**

315
316 **LDAK:** www.ldak.org

317 **PLINK:** www.cog-genomics.org/plink2

318 **SHAPEIT:** www.shapeit.fr

319 **IMPUTE2:** mathgen.stats.ox.ac.uk/impute/impute_v2.html

320 **DHS annotations:**

321 [hgdownload.cse.ucsc.edu/goldenPath/hg19/encodeDCC/wgEncodeRegDnaseClustered/wgEncodeRegDnaseClusteredV](http://hgdownload.cse.ucsc.edu/goldenPath/hg19/encodeDCC/wgEncodeRegDnaseClustered/wgEncodeRegDnaseClusteredV3.bed.gz)
322 [3.bed.gz](http://hgdownload.cse.ucsc.edu/goldenPath/hg19/encodeDCC/wgEncodeRegDnaseClustered/wgEncodeRegDnaseClusteredV3.bed.gz)

323 **RefSeq annotations:** <http://hgdownload.cse.ucsc.edu/goldenPath/hg19/database/refGene.txt.gz>

324 325 **Methods**

326
327 Methods and any associated references are available in the online version of the paper.

328 329 **Code Availability**

330
331 Step-by-step instructions for estimating h^2_{SNP} starting from raw genotype data, as well as for performing our other
332 analyses, are provided in the Supplementary Note.

333 334 **Data Availability**

335
336 In total, we analyze data from 40 cohorts; 25 of these were downloaded (after completing a data access request) from
337 the European Genome-phenome Archive or dbGaP, while the remaining 15 (which include the 8 UCLEB cohorts) were
338 obtained direct from the relevant custodians. Full details of the cohorts (with accession codes where applicable) are
339 provided in the Supplementary Material.

340 341 **Acknowledgments**

342
343 Access to Wellcome Trust Case Control Consortium data was authorized as work related to the project "Genome wide
344 association study of susceptibility and clinical phenotypes in epilepsy," while access to Children's Hospital of
345 Philadelphia (CHOP) data was granted under Project 49228-1, "Assumptions underlying estimates of SNP Heritability."
346 We thank Anne Molloy, James Mills and Lawrence Brody for permission to use genotype data from the Trinity College
347 Dublin Student Study,⁴² and Sarah Langley for help accessing the CHOP data. This work is funded by the UK Medical
348 Research Council under grant MR/L012561/1 (awarded to D.S.), by the British Heart Foundation under grant
349 RG/10/12/28456 (the UCLEB Consortium), and supported by researchers at the National Institute for Health Research
350 (NIHR) University College London Hospitals Biomedical Research Centre. N.C. is an ESPOD Fellow from the
351 European Molecular Biology Laboratory, European Bioinformatics Institute, and Wellcome Trust Sanger Institute. S.N.
352 is a Wellcome Trust Senior Research Fellow in Basic Biomedical Science and is also supported by the NIHR
353 Cambridge Biomedical Research Centre. Analyses were performed with the use of the UCL Computer Science Cluster
354 and the help of the CS Technical Support Group, as well as the use of the UCL Legion High Performance Computing
355 Facility (Legion@UCL) and associated support services.

356 357 **Author Contributions**

358
359 D.S. and N.C. performed the analyses. D.S. and D.J.B. wrote the manuscript with assistance from N.C., M.R.J., S.N.
360 and members of the UCLEB Consortium.

361 362 **Competing Financial Interests**

363
364 The authors declare no competing financial interests.

365
366

367 **References**

368

- 369 1. Yang, J. *et al.* Common SNPs explain a large proportion of the heritability for human height. *Nat. Genet.* **42**,
370 565–569 (2010).
- 371 2. Maher, B. Personal Genomes: the case of the missing heritability. *Nature* **456**, 18–21 (2008).
- 372 3. Speed, D. *et al.* Describing the genetic architecture of epilepsy through heritability analysis. *Brain* **137**, 2680–
373 2689 (2014).
- 374 4. Henderson, C., Kempthorne, O., Searle, S. & von Krosigk, C. The Estimation of Environmental and Genetic
375 Trends from Records Subject to Culling. *Biometrics* **15**, 192–218 (1959).
- 376 5. Falconer, D. & Mackay, T. *Introduction to Quantitative Genetics (4th Edition)*. (Longman, 1996).
- 377 6. Yang, J. *et al.* Genomic partitioning of genetic variation for complex traits using common SNPs. *Nat. Genet.* **43**,
378 519–525 (2011).
- 379 7. Gusev, A. *et al.* Partitioning Heritability of Regulatory and Cell-Type-Specific Variants across 11 Common
380 Diseases. *Am. J. Hum. Genet.* **95**, 535–552 (2014).
- 381 8. Lee, S. H., Yang, J., Goddard, M. E., Visscher, P. M. & Wray, N. R. Estimation of pleiotropy between complex
382 diseases using single-nucleotide polymorphism-derived genomic relationships and restricted maximum
383 likelihood. *Bioinformatics* **28**, 2540–2 (2012).
- 384 9. Speed, D., Hemani, G., Johnson, M. & Balding, D. Improved heritability estimation from genome-wide SNP
385 data. *Am. J. Hum. Genet.* **91**, 1011–1021 (2012).
- 386 10. Bulik-Sullivan, B. *et al.* LD Score Regression Distinguishes Confounding from Polygenicity in Genome-Wide
387 Association Studies. *Nat. Genet.* **47**, 291–295 (2014).
- 388 11. Bulik-Sullivan, B. Relationship between LD Score and Haseman-Elston Regression. *bioRxiv* 18283 (2015).
389 doi:10.1101/018283
- 390 12. Corbeil, R. & Searle, S. Restricted Maximum Likelihood (REML) Estimation of Variance Components in the
391 Mixed Model. *Technometrics* **18**, 31–38 (1976).
- 392 13. Golan, D., Lander, E. S. & Rosset, S. Measuring missing heritability: Inferring the contribution of common
393 variants. *Proc. Natl. Acad. Sci.* **111**, E5272–E5281 (2014).
- 394 14. Lee, S. H. *et al.* Estimation of SNP heritability from dense genotype data. *Am. J. Hum. Genet.* **93**, 1151–1155
395 (2013).
- 396 15. Yang, J. *et al.* Genetic variance estimation with imputed variants finds negligible missing heritability for human
397 height and body mass index. *Nat. Genet.* **47**, 1114–1120 (2015).
- 398 16. Ek, W. *et al.* Germline Genetic Contributions to Risk for Esophageal Adenocarcinoma, Barrett’s Esophagus, and
399 Gastroesophageal Reflux. *J. Natl. Cancer Inst.* **105**, 1711–1718 (2013).
- 400 17. Bevan, S. *et al.* Genetic heritability of ischemic stroke and the contribution of previously reported candidate
401 gene and genomewide associations. *Stroke* **43**, 3161–3167 (2012).
- 402 18. Keller, M. *et al.* Using genome-wide complex trait analysis to quantify ‘missing heritability’ in Parkinson’s
403 disease. *Hum. Mol. Genet.* **21**, 4996–5009 (2012).
- 404 19. Yin, X. *et al.* Common variants explain a large fraction of the variability in the liability to psoriasis in a Han
405 Chinese population. *BMC Genomics* **15**, (2014).
- 406 20. Lee, S. *et al.* Estimating the proportion of variation in susceptibility to schizophrenia captured by common
407 SNPs. *Nat. Genet.* **44**, 247–250 (2012).
- 408 21. Chen, G. *et al.* Estimation and partitioning of (co)heritability of inflammatory bowel disease from GWAS and
409 immunochip data. *Hum. Mol. Genet.* **23**, 4710–4720 (2014).

- 410 22. Stahl, E. *et al.* Bayesian inference of the polygenic architecture of rheumatoid arthritis. *Nat. Genet.* **44**, 483–489
411 (2012).
- 412 23. Robinson, E. *et al.* The genetic architecture of pediatric cognitive abilities in the Philadelphia
413 Neurodevelopmental Cohort. *Mol. Psychiatry* **20**, 454–458 (2015).
- 414 24. Shah, T. *et al.* Population Genomics of Cardiometabolic Traits: Design of the University College London-
415 London School of Hygiene and Tropical Medicine-Edinburgh-Bristol (UCLEB) Consortium. *PLoS One* **8**,
416 e71345 (2013).
- 417 25. Voight, B. *et al.* The Metabochip, a Custom Genotyping Array for Genetic Studies of Metabolic,
418 Cardiovascular, and Anthropometric Traits. *PLoS Genet.* **8**, e1002793 (2012).
- 419 26. Dempster, E. & Lerner, I. Heritability of threshold characters. *Genetics* **35**, 212–236 (1950).
- 420 27. Lee, S., Wray, N., Goddard, M. & Visscher, P. Estimating missing heritability for disease from genome-wide
421 association studies. *Am. J. Hum. Genet.* **88**, 294–305 (2011).
- 422 28. Yang, J., Lee, S. H., Goddard, M. E. & Visscher, P. M. GCTA: A tool for genome-wide complex trait analysis.
423 *Am. J. Hum. Genet.* **88**, 76–82 (2011).
- 424 29. K. Pruit, Brown, G. & Tatusova, T. The NCBI handbook [Internet]. (2002).
- 425 30. Finucane, H. *et al.* Partitioning heritability by functional annotation using genome-wide association summary
426 statistics. *Nat. Genet.* **47**, 1228–1235 (2015).
- 427 31. Hastie, T., Tibshirani, R. & Friedman, J. *The Elements of Statistical Learning*. (Springer, 2001).
- 428 32. Habier, D., Fernando, R. L., Kizilkaya, K. & Garrick, D. J. Extension of the bayesian alphabet for genomic
429 selection. *BMC Bioinformatics* **12**, 186 (2011).
- 430 33. Lippert, C. *et al.* FaST linear mixed models for genome-wide association studies. *Nat. Methods* **8**, 833–835
431 (2011).
- 432 34. Zhou, X. & Stephens, M. Efficient multivariate linear mixed model algorithms for genome-wide association
433 studies. *Nat. Methods* **11**, 407–9 (2014).
- 434 35. Yang, J., Zaitlen, N., Goddard, M., Visscher, P. & Price, A. Advantages and pitfalls in the application of mixed-
435 model association methods. *Nat. Genet.* **46**, 100–106 (2014).
- 436 36. Loh, P.-R. *et al.* Efficient Bayesian mixed-model analysis increases association power in large cohorts. *Nat.*
437 *Genet.* **47**, 284–290 (2015).
- 438 37. Cross-Disorder Group of the Psychiatric Genomics Consortium. Genetic relationship between five psychiatric
439 disorders estimated from genome-wide SNPs. *Nat. Genet.* **45**, 984–994 (2013).
- 440 38. Bulik-Sullivan, B. *et al.* An atlas of genetic correlations across human diseases and traits. *Nat. Genet.* **47**, 1236–
441 1241 (2015).
- 442 39. Gazal, S. *et al.* Linkage disequilibrium dependent architecture of human complex traits reveals action of
443 negative selection. (2016).
- 444 40. The ENCODE Project Consortium. An integrated encyclopedia of DNA elements in the human genome. *Nature*
445 **489**, 57–74 (2012).
- 446 41. Kumar, S., Feldman, M., Rehkopf, D. & Tuljapurkar, S. Limitations of GCTA as a solution to the missing
447 heritability problem. *PNAS* **113**, E61–E70 (2015).
- 448 42. Molloy, A. *et al.* A Common Polymorphism in HIBCH Influences Methylmalonic Acid Concentrations in Blood
449 Independently of Cobalamin. *Am. J. Hum. Genet.* **5**, 869–882 (2016).

450 **Figure Legends**

451
452
453
454
455
456
457
458
459
460
461
462
463
464
465
466
467
468
469
470
471
472
473
474
475
476
477
478
479
480
481
482
483
484
485
486
487
488
489
490
491
492
493
494
495
496
497
498
499
500
501
502
503
504
505
506
507
508
509
510
511

Figure 1 - Comparison of the GCTA and LDAK Models. Region 1 contains five SNPs in low LD (lighter colors indicate weaker pairwise correlations). Each SNP contributes unique genetic variation, reflected by SNP weights close to one. Region 2 contains five SNPs in high LD (strong correlations). The total genetic variation tagged by the region is effectively captured by two of the SNPs, and so the others receive zero weight. Under the GCTA Model, the regions are expected to contribute heritability proportional to their numbers of SNPs, here equal. Under the LDAK Model, they are expected to contribute proportional to their sums of SNP weights, here in the ratio 4.6:1.9. Note that the expected heritability can also depend on the allele frequencies and genotype certainty of the SNPs, but for simplicity, these factors are ignored here.

Figure 2 - (a) Relationship between heritability and MAF. The parameter α specifies the assumed relationship between heritability and MAF: in human genetics, $\alpha=-1$ is typically used (solid blue line), while in animal and plant genetics, $\alpha=0$ is more common (orange); we instead found $\alpha=-0.25$ (red) provides a better fit to real data. The gray bars report (relative) estimates of the per-SNP heritability for $MAF<0.1$ and $MAF>0.1$ SNPs, averaged across the 19 GWAS traits (vertical lines provide 95% confidence intervals); the dashed lines indicate the per-SNP heritability predicted by each α . **(b) Determining best-fitting α for the GWAS traits.** We compare α based on likelihood; higher likelihood indicates better-fitting α . Lines report log likelihoods from LDAK for seven values of α , relative to the highest observed. Line colors indicate the seven trait categories, while the black line reports averages.

Figure 3 - (a) Relative estimates of h^2_{SNP} for the GWAS traits. h^2_{SNP} estimates from LDSC, GCTA-MS (SNPs partitioned by MAF), GCTA-LDMS (SNPs partitioned by LD and MAF) and LDAK are reported relative to those from GCTA. For versions of GCTA and LDAK, we use $\alpha=-0.25$ (see main text for explanation of α). Line colors indicate the seven trait categories; the black line reports the (inverse variance weighted) averages, with gray boxes providing 95% confidence intervals for these averages. Numerical values are provided in Supplementary Table 3. **(b) Simulation studies can be misleading.** Phenotypes are simulated with 1000 causal SNPs and $h^2_{SNP}=0.8$ (black horizontal line), then analyzed using GCTA, GCTA-MS, GCTA-LDMS, LDAK and LDAK-MS (LDAK with SNPs partitioned by MAF). Bars report average h^2_{SNP} across 200 simulated phenotypes (vertical lines provide 95% confidence intervals). **Left:** copying the study of Yang *et al.*,¹⁵ causal SNP effect sizes are sampled from $N(0,1)$, similar to the GCTA Model. **Right:** causal SNP effect sizes are sampled from $N(0,w_j)$, similar to the LDAK Model.

Figure 4 - Comparing the GCTA and LDAK Models for the GWAS traits: We partition SNPs into low- or high-LD, with the low-LD tranche containing either 50% (left) or 25% (right) of SNPs. For each partition, the horizontal red and black lines indicate the predicted contribution of the low-LD tranche to h^2_{SNP} under the GCTA and LDAK Models, respectively. Vertical lines provide point estimates and 95% confidence intervals for the contribution of the low-LD tranche to h^2_{SNP} , estimated assuming the GCTA Model. Line colors indicate the seven trait categories, while the black lines provide the (inverse variance weighted) averages.

Figure 5 - Enrichment of SNP Classes. Block 1 reports the contributions to h^2_{SNP} of DNaseI hypersensitivity sites (DHS), estimated under the GCTA Model with $\alpha=-1$ (see main text for explanation of α). The vertical lines provide point estimates and 95% confidence intervals for each trait, and for the (inverse variance weighted) average; for 3 of the traits, the point estimate is above 100%, as was also the case for Gusev *et al.*⁷ Block 2 repeats this analysis, but now assuming the LDAK Model with $\alpha=-0.25$. Blocks 3 & 4 estimate the contribution of "genic SNPs" (those inside or within 2kb of an exon) and "inter-genic SNPs" (further than 125kb from an exon), again assuming the LDAK Model with $\alpha=-0.25$. To assess enrichment, estimated contributions are compared to those expected under the GCTA or LDAK Model, as appropriate (horizontal lines).

Figure 6 - Varying quality control for the UCLEB traits. We consider three SNP filterings: 353K high-quality common SNPs (information score >0.99 , $MAF>0.01$), 8.8M common SNPs ($MAF>0.01$) and all 17.3M SNPs ($MAF>0.0005$). **(a)** Blocks indicate SNP filtering; bars report (inverse variance weighted) average estimates of h^2_{SNP} using LDAK (vertical lines provide 95% confidence intervals). Bar color indicates the value of α used. For Blocks 1, 2 & 3, h^2_{SNP} is estimated using the non-partitioned model. For Block 4, SNPs are partitioned by MAF; we find this is necessary when rare SNPs are included, and also allows estimation of the contribution of $MAF<0.01$ SNPs (hatched areas). **(b)** Bars report our final estimates of h^2_{SNP} for height, body mass index and QT interval, the three traits for which common SNP heritability has been previously estimated with reasonable precision⁶ (orange lines mark the 95% confidence intervals from these previous studies). Bar colors now indicate SNP filtering; all estimates are based on $\alpha=-0.25$, using either a non-partitioned model (red and blue bars) or with SNPs partitioned by MAF (purple bars).

Collection	Trait (Disease Prevalence, %)	n	m	$\sum_{j=1}^m w_j$	h^2_{GWAS}	Estimates of h^2_{SNP} & SDs			
						Previous		LDAK	
Welcome Trust Case Control Consortium 1 (WTCCC 1)	Bipolar Disorder (0.5)	1840+2913	2729	79K	0.02	0.24 ⁷ □ □	0.04	0.35	0.03
	Coronary Artery Disease (6)	1907+2918	2739	80K	0.03	0.25 ⁷	0.06	0.40	0.06
	Crohn's Disease (0.5)	1691+2905	2724	79K	0.21	0.26 ²¹ □	0.01	0.32	0.03
	Hypertension (5)	1918+2916	2740	80K	<0.01	0.33 ⁷	0.06	0.46	0.06
	Rheumatoid Arthritis (0.5)	1846+2918	2736	80K	0.19	0.09 ⁷	0.03	0.21	0.03
	Type 1 Diabetes (0.5)	1941+2907	2732	80K	0.27	0.13 ⁷	0.03	0.31	0.02
	Type 2 Diabetes (8)	1896+2917	2736	80K	0.08	0.42 ⁷	0.07	0.54	0.07
Welcome Trust Case Control Consortium 2 (WTCCC 2)	Barrett's Oesophagus (1.6)	1861+5138	3831	116K	<0.01	0.25 ¹⁶	0.05	0.32	0.04
	Ischaemic Stroke (2)	3769+5139	3797	115K	<0.01	0.25 ¹⁷ □	0.03	0.34	0.03
	Parkinson's Disease (0.2)	1687+5136	3820	116K	0.03	0.27 ¹⁸	0.05	0.20	0.03
	Psoriasis (0.5)	2267+5143	3815	116K	0.21	0.35 ¹⁹	0.06	0.34	0.02
	Schizophrenia (1)	2068+2615	3481	111K	0.07	0.23 ²⁰	0.01	0.30	0.04
	Ulcerative Colitis (0.2)	2614+5327	4062	115K	0.12	0.19 ²¹	0.01	0.28	0.02
WTCCC 2+	Celiac Disease (1)	2492+7376	2682	88K	0.29	0.33 ²²	0.04	0.35	0.02
	Multiple Sclerosis (0.1)	8553+5667	3702	113K	0.17	0.17 ⁷	0.01	0.24	0.01
	Partial Epilepsy (0.3)	1217+5152	3399	108K	<0.01	0.33 ³ □	0.05	0.27	0.04
RPTB	Pulmonary Tuberculosis (4)	5142+5283	2987	102K	<0.01	None	Found	0.26	0.03
Blue Mountains	Intraocular Pressure	2235	4149	125K	0.02	None	Found	0.38	0.17
CHOP	Wide-Range Achievement Test	3747	2593	88K	<0.01	0.43 ²³	0.1	0.21	0.09
UCLEB	23 Quantitative Traits	6458 to 11005	353	39K	- - -	Supplementary Table 1			

514
515
516
517
518
519
520
521
522
523
524
525
526
527
528
529
530
531
532
533
534
535
536
537

Table 1: Properties of datasets and estimates of h^2_{SNP} . n = sample size (cases+controls), m = number of SNPs, $\sum_j w_j$ = sum of SNP weights which can be interpreted as an effective number of independent SNPs. All values are post quality control; values for m and $\sum_j w_j$ are rounded to the nearest K (thousand). For UCLEB, m and $\sum_j w_j$ refer to our main analysis, which considers only high-quality, common SNPs. The final column provides our best estimates of h^2_{SNP} from common SNPs, computed using LDAK with $\alpha=-0.25$ (see main text for explanation of α). For comparison, we include previously published estimates of h^2_{SNP} (note that the previous analyses for rheumatoid arthritis, type 1 diabetes and multiple sclerosis excluded major histocompatibility SNPs, which we estimate contribute 0.07, 0.20 and 0.05, respectively), as well as h^2_{GWAS} , the proportion of phenotypic variance explained by SNPs reported as GWAS significant ($P < 5 \times 10^{-8}$). For disease traits, estimates of h^2_{SNP} and h^2_{GWAS} have been converted to the liability scale assuming the stated prevalence.

538
539
540

541 **Online Methods**

542

543

544

545

546

547

548

549

550

551

552

553

The Supplementary Note summarizes the different analyses we performed, and the conclusions we drew from each. In general, we assume there are n individuals, recorded for p covariates and genotyped (either directly or via imputation) for m SNPs: the length- n vector \mathbf{Y} contains phenotypic values, the $n \times p$ matrix \mathbf{Z} contains covariates, while the $n \times m$ matrix \mathbf{S} contains (expected) allele counts.

Information score r_j : Let the vector $\mathbf{S}_j = (S_{1,j}, \dots, S_{n,j})^T \in [0,2]^n$, denote the allele counts for SNP j (i.e., \mathbf{S}_j is Column j of \mathbf{S}). Our information score r_j estimates the squared correlation between \mathbf{S}_j and $\mathbf{G}_j = (G_{1,j}, \dots, G_{n,j})^T \in \{0,1,2\}^n$, the true genotypes for SNP j . When using imputed data, \mathbf{G}_j is typically not known; instead for each individual we have a triplet of state probabilities $p_{i,j,0}, p_{i,j,1}, p_{i,j,2}$, where $p_{i,j,g} = P(G_{i,j}=g)$ and $p_{i,j,0} + p_{i,j,1} + p_{i,j,2} = 1$. Therefore, we define r_j by taking expectations over the 3^n possible realizations of \mathbf{G}_j :

$$r_j = \frac{E[\sum_{i=1}^n (S_{i,j} - \bar{S}_j)(G_{i,j} - \bar{G}_j)]^2}{(\sum_{i=1}^n (S_{i,j} - \bar{S}_j)^2) E[\sum_{i=1}^n (G_{i,j} - \bar{G}_j)^2]}, \quad \text{where } \bar{S}_j = \frac{1}{n} \sum_{i=1}^n S_{i,j} \quad \text{and} \quad \bar{G}_j = \frac{1}{n} \sum_{i=1}^n G_{i,j}$$

554

555

556

557

\mathbf{S}_j is known, so computing $\sum_i (S_{i,j} - \bar{S}_j)^2$ is straightforward. The two expectations can also be calculated explicitly:

558

$$E[\sum_{i=1}^n (S_{i,j} - \bar{S}_j)(G_{i,j} - \bar{G}_j)] = \sum_i (S_{i,j} - \bar{S}_j) E[G_{i,j} - \mu] = \sum_i (S_{i,j} - \bar{S}_j) (p_{i,j,1} + 2p_{i,j,2} - \mu),$$

559

560

$$E[\sum_{i=1}^n (G_{i,j} - \bar{G}_j)^2] = \sum_i E[(G_{i,j} - \mu)^2] = \sum_i [p_{i,j,0}(-\mu)^2 + p_{i,j,1}(1-\mu)^2 + p_{i,j,2}(2-\mu)^2],$$

561

where

$$\mu = E[\bar{G}_j] = \frac{1}{n} \sum_i (p_{i,j,1} + 2p_{i,j,2}).$$

For our analyses, we use expected allele counts (dosages), so

562

$S_{i,j} = p_{i,j,1} + 2p_{i,j,2}$. In this case,

$$E[\sum_i (S_{i,j} - \bar{S}_j)(G_{i,j} - \bar{G}_j)] = \sum_i (S_{i,j} - \bar{S}_j)^2$$

and so the score reduces to

563

564

565

566

$r_j = \sum_i (S_{i,j} - \bar{S}_j)^2 / \sum_i (G_{i,j} - \bar{G}_j)^2$ For a directly genotyped SNP, each triplet of state probabilities will be (1,0,0), (0,1,0) or (0,0,1), which will result in $S_{i,j} = G_{i,j}$ for all i and $r_j=1$; so for these, in place of r_j , we use the metric $r2_type2$ reported by IMPUTE2.⁴³ Additional details on our information score are provided in Supplementary Figure 20.

567

568

569

570

Estimating h^2_{SNP} : We first construct the $n \times m$ genotype matrix \mathbf{X} , by centering and scaling the allele counts for each SNP according to $X_{ij} = (S_{ij} - 2f_j) \times [2f_j(1-f_j)]^{\alpha/2}$, where $f_j = \sum_i S_{ij} / 2n$. If w_i and r_j denote the LD weight⁹ and information score for SNP j then the LDK Model for estimating SNP heritability $h^2_{\text{SNP}} = \sigma_g^2 / (\sigma_g^2 + \sigma_e^2)$ is:

571

$$Y_i = \sum_{k=1}^p \theta_k Z_{i,k} + \sum_{j=1}^m \beta_j X_{i,j} + e_i, \quad \text{with } \beta_j \sim N(0, r_j w_j \sigma_g^2 / W), \quad e_i \sim N(0, \sigma_e^2) \quad \text{and}$$

572

573

$$W = r_j w_j [2f_j(1-f_j)]^{1+\alpha}. \quad (2)$$

574

575

576

577

578

θ_k denotes the fixed-effect coefficient for the k th covariate, β_j and e_i are random-effects indicating the effect size of SNP j and the noise component for Individual i , while σ_g^2 and σ_e^2 are interpreted as genetic and environmental variances, respectively. Note that the introduction of r_j is an addition to the model we proposed in 2012.⁹ Model (2) is equivalent to assuming:^{44,45}

579

580

581

582

583

584

585

$$Y \sim N(\mathbf{Z}\boldsymbol{\theta}, \mathbf{K}\sigma_g^2 + \mathbf{I}\sigma_e^2), \quad \text{with } \mathbf{K} = \frac{\mathbf{X}\boldsymbol{\Omega}\mathbf{X}^T}{W}, \quad (3)$$

where \mathbf{I} is an $n \times n$ identity matrix and $\boldsymbol{\Omega}$ denotes a diagonal matrix with diagonal entries $(r_1 w_1, \dots, r_m w_m)$. The kinship matrix \mathbf{K} , also referred to as a genetic relationship matrix (GRM)¹ or genomic similarity matrix (GSM),⁴⁶ consists of average allelic correlations across the SNPs (adjusted for LD and genotype certainty). Model (3) is typically solved using REstricted Maximum Likelihood (REML), which returns estimates of $\theta_1, \dots, \theta_p, \sigma_g^2$ and σ_e^2 .¹²

586

587

588

The heritability of SNP j can be estimated by $h^2 = \beta_j^2 \text{Var}(X_j) / \text{Var}(Y)$, which under Model (2), and assuming Hardy-Weinberg Equilibrium,^{47,48} has expectation

$$E[h_j^2] = \frac{E[\beta_j^2] \times \text{Var}(X_j)}{\text{Var}(Y)} = \frac{r_j w_j \sigma_g^2 / W \times [2f_j(1-f_j)]^{1+\alpha}}{\text{Var}(Y)}. \quad (4)$$

If P_1 and P_2 index two sets of SNPs of size $|P_1|$ and $|P_2|$, then under the LDAK Model, they are expected to contribute

heritability in the ratio $W_1:W_2$, where $W_l = \sum_{j \in P_l} r_j w_j [2f_j(1-f_j)]^{1+\alpha}$. The GCTA Model corresponds to setting

$w_j = r_j = 1$, in which case $W_l = \sum_{j \in P_l} [2f_j(1-f_j)]^{1+\alpha}$. Most applications of GCTA have further assumed $\alpha = -1$, so that $W_l = |P_l|$, which corresponds to the assumption that SNP sets are expected to contribute heritability proportional to the number of SNPs they contain.

Model (2) assumes that all effect-sizes can be described by a single prior distribution. This assumption is relaxed by SNP partitioning. Suppose that the SNPs are divided into tranches P_1, \dots, P_L of sizes $|P_1|, \dots, |P_L|$; typically these will partition the genome, so that each SNP appears in exactly one tranche and $\sum_l |P_l| = m$, but this is not required. This correspond to generalizing Model (2), so that SNPs in Tranche l have effect-size prior distribution $\beta_j \sim N(0, r_j w_j \sigma_l^2 / W_l)$. Letting $\Sigma = \sigma_1^2, \dots, \sigma_L^2$, then $h_{\text{SNP}}^2 = \Sigma / (\Sigma + \sigma_e^2)$, while σ_l^2 / Σ represents the contribution to h_{SNP}^2 of SNPs in Tranche l . This model can equivalently be expressed as $\mathbf{Y} \sim N(\mathbf{Z}\mathbf{0}, \mathbf{K}_1 \sigma_1^2 + \dots + \mathbf{K}_L \sigma_L^2 + \mathbf{I} \sigma_e^2)$, where \mathbf{K}_l represents allele correlations across the SNPs in Tranche l .

For analyses under the LDAK Model, we used LDAK v.5; for analyses under the GCTA Model, we used GCTA v.1.26. For about a third of GCTA-LDMS analyses, the GCTA REML solver failed with the error "information matrix is not invertible," in which case we rerun using LDAK (while the GCTA and LDAK solvers are both based on Average Information REML,^{28,49} subtle differences mean that when using a large number of tranches, one might complete while the other fails). For the few occasions when both solvers failed, we instead used "GCTA-LD" (i.e., SNPs divided only by LD, rather than by LD and MAF), which we found gave very similar results to GCTA-LDMS for traits where both completed (Supplementary Fig. 7). For diseases, we converted estimates of h_{SNP}^2 to the liability scale based on the observed case-control ratio and assumed prevalence.^{26,27} In general, we copied the prevalences used by previous studies; however for tuberculosis, where no previous estimate of h_{SNP}^2 is available, we derived an estimate of prevalence from World Health Organization data⁵⁰ (see Supplementary Note).

LDSC: Originally designed as a way to quantify confounding in a GWAS, LDSC¹⁰ also provides a method for estimating h_{SNP}^2 , which requires only summary statistics from single-SNP analysis (rather than raw genotype and phenotype data). LDSC is based on the principal that in a single-SNP analysis, the $X^2(1)$ test statistic for SNP j has expected value $E[X^2(1)] = 1 + n h_j^2 + n \sum_{k \neq j} r_{j,k}^2 h_k^2 + n a_j$, where $r_{j,k}^2$ denotes the squared correlation between SNPs j and k , while a_j represents bias due to confounding factors (e.g., population structure and familial relatedness).¹⁰ Under a polygenic model where every SNP is expected to contribute equally (i.e., $E[h_j^2] = h_{\text{SNP}}^2/m$), and the (widely-used) assumption that the bias is constant across SNPs ($a_j = a$), we have $E[X^2(1)] = 1 + n l_j h_{\text{SNP}}^2 / m + n a$, where $l_j = 1 + \sum_{k \neq j} r_{j,k}^2$ is referred to as the LD Score of SNP j (as it is not feasible to compute pairwise correlations across all SNPs, in practice these are approximated using a sliding window of, say, 1 centiMorgan). Therefore, LDSC estimates h_{SNP}^2 and a by regressing test statistics on LD Scores. In the absence of confounding ($a=0$), LDSC can be viewed as estimating h_{SNP}^2 under the GCTA Model with $\alpha = -1$ (as this satisfies the assumption that every SNP is expected to contribute equal heritability). As the authors of LDSC point out,¹⁰ it is straightforward to accommodate alternative relationships between $E[h_j^2]$ and MAF (i.e., $\alpha \neq -1$) by changing how genotypes are scaled when computing LD Scores, and potentially genotype certainty could be accommodated. However, the similarity with the GCTA Model appears intrinsic to LDSC; while the assumption that heritability is independent of LD can be relaxed via SNP partitioning,³⁹ we can not envisage how the method could be modified to accommodate the LDAK SNP weights. For LDSC analyses, we used LDSC v.1.0.0 both for calculating LD Scores and estimating h_{SNP}^2 .

Accommodating very large effect loci: Equation (2) assumes that all SNP effect sizes can be modeled by a single Gaussian distribution. Estimates are generally robust to violations of this assumption,⁹ but problems can occur when individual SNPs have very large effect sizes, because a single Gaussian distribution cannot accommodate both these SNPs and the very many with small effect sizes. This is a common concern when analyzing autoimmune traits for which the major histocompatibility complex (MHC) can contribute substantial heritability. In response to this problem, some authors exclude MHC SNPs from analyses.^{7,28,51,52} Another approach is to model effect sizes as a mixture of Gaussians,^{53,54} but this is not computationally feasible for millions of SNPs and many thousands of individuals. Therefore, our proposed strategy is to first identify SNPs with $P < 10^{-20}$ from single-SNP analysis, to prune these using a correlation squared threshold of 0.5, then to include those which remain as fixed-effect covariates. Thus in place of Equation (3), we assume $\mathbf{Y} \sim N(\mathbf{Z}\mathbf{0} + \mathbf{T}\mathbf{\Phi}, \mathbf{K}\sigma_g^2 + \mathbf{I}\sigma_e^2)$, where columns of the matrix \mathbf{T} contain allele counts of the highly-associated SNPs (i.e., \mathbf{T} is a submatrix of \mathbf{S}), and the vector $\mathbf{\Phi}$ represents their effect sizes. In contrast to standard (non-SNP) covariates, the variance explained by \mathbf{T} counts towards SNP heritability: $h_{\text{SNP}}^2 = (\sigma_g^2 + \sigma_T^2) / (\sigma_g^2 + \sigma_e^2)$

647 $\sigma_T^2 + \sigma_e^2$), where $\sigma_T^2 = (\mathbf{T}\Phi)^T(\mathbf{T}\Phi)$. Supplementary Figures 21 & 22 provides further details. In particular, we
648 appreciate that our definition of highly-associated is somewhat arbitrary, so we confirm that estimates of h_{SNP}^2 are
649 almost unchanged if instead we use $P < 5 \times 10^{-8}$.
650

651 **Datasets and phenotypes:** When searching for GWAS datasets, we preferred those with sample size at least 4000 to
652 ensure reasonable precision of h_{SNP}^2 .⁵⁵ In total, our datasets were constructed from 40 independent cohorts, all of which
653 have been previously described (see Supplementary Tables 11 & 12 for references and details of how cohorts were
654 merged to form datasets). For the UCLEB data, there were in total 28 quantitative traits with measurements recorded for
655 at 7000 individuals. For each of these, we quantile normalized, then applied a test for inflation due to genotyping errors
656 (Supplementary Fig. 13). Specifically, our test, inspired by Bhatia *et al.*⁵⁶ and valid for quantitative phenotypes where
657 individuals are recruited from multiple cohorts, first estimates h_{SNP}^2 using only pairs of individuals in different cohorts,
658 then using only pairs of individuals in the same cohort; a significant difference between the two estimates indicates
659 possible inflation due to genotyping errors. We excluded five traits that showed evidence of inflation ($P < 0.05/28$),
660 leaving us with 23: height, weight, body mass index, waist circumference, forced vital capacity, one second forced vital
661 capacity, systolic blood pressure (adjusted), diastolic blood pressure (adjusted), PR Interval, QT Interval, Corrected QT
662 Interval, QRS Voltage Product, Sokolow Lyon, glucose, insulin, total cholesterol (adjusted), LDL cholesterol (adjusted),
663 triglyceride (adjusted), viscosity, fibrinogen, Interleukin 6, C-reactive Protein and haemoglobin. Approximately 40% of
664 individuals were receiving medication to reduce blood pressure, 25% to reduce lipid levels, so where indicated,
665 phenotypes had been adjusted for this: for individuals on medication, their raw measurements had been increased either
666 by adding on (blood pressure) or scaling by (lipid levels) a constant.^{57,58} We note that some pairs of traits are highly
667 correlated. However, as the overall correlation is not that extreme (we estimate the effective number of independent
668 traits to be about 15), and most of our UCLEB analyses serve to support conclusions drawn from the GWAS traits, we
669 decide to retain all 23 traits (rather than, say, consider only a subset). See the Supplementary Note for further details on
670 phenotyping.
671

672 **Quality control:** We processed each of the 40 cohorts in identical fashion; see the Supplementary Note for full details.
673 In summary, after excluding apparent population outliers, samples with extreme missingness or heterozygosity, and
674 SNPs with $\text{MAF} < 0.01$, $\text{call-rate} < 0.95$ or $P < 10^{-6}$ from a test for Hardy-Weinberg Equilibrium, we phased using
675 SHAPEIT⁵⁹ then imputed using IMPUTE2⁴³ and the 1000 Genome Phase 3 (2014) reference panel.⁶⁰ When
676 merging cohorts to construct the GWAS datasets, we retained only autosomal SNPs which in all cohorts have
677 $\text{MAF} > 0.01$ and $r_j > 0.99$ (using IMPUTE2 *r2_type2* in place of r_j for directly genotyped SNPs). For the 8 UCLEB
678 cohorts, we applied these filters only after merging. We only relax quality control for the analyses of the UCLEB data
679 where we explicitly examine the consequences of including lower-quality and rare SNPs. When possible, the matrix \mathbf{S}
680 contains expected allele counts (dosages); i.e., $S_{ij} = p_{i,j,1} + 2p_{i,j,2}$, where $p_{i,j,1}$ and $p_{i,j,2}$ denote the probabilities of allele
681 counts 1 and 2, respectively. If hard genotypes are required, for example when using LDSC to compute LD Scores,¹⁰
682 we round S_{ij} to the nearest integer. As this was only necessary when considering high-quality SNPs ($r_j > 0.99$), we expect
683 this rounding to have negligible impact on results. For each trait, Table 1 reports m , the total number of SNPs after

684 imputation, and $\sum_{j=1}^m w_j$, the sum of SNP weights; the aim of these weights is to remove duplication of signal due to
685 LD and their sum can loosely be interpreted as an effective number of independent SNPs. For the GWAS datasets, $\sum_j w_j$
686 ranges from 79K to 125K. By contrast, when restricted to only high-quality SNPs, the UCLEB data has $\sum_j w_j = 39\text{K}$,
687 reflecting that the Metabochip directly captures a much smaller amount of genetic variation than standard genome-wide
688 SNP arrays.
689

690 When analyzing quantitative traits, genotyping errors will tend only to be a concern when there are systematic
691 differences between phenotypes across cohorts, and this is something we are able to explicitly test (Supplementary Fig.
692 13). However, for disease traits, when cases and controls have been genotyped separately (as is the design of most of
693 our GWAS datasets), any errors will almost certainly correlate with phenotype and therefore cause inflation of
694 h_{SNP}^2 .^{9,27} To test the effectiveness of our quality control for the GWAS traits, we construct a pseudo case-control study
695 using two control cohorts; we confirm that the resulting estimate of h_{SNP}^2 is not significantly greater than zero,
696 suggesting that the quality control steps we use for the GWAS datasets are sufficiently strict (Supplementary Note).
697

698 Accurate estimation of h_{SNP}^2 requires samples of unrelated individuals with similar ancestry. Prior to imputation, we
699 removed ethnic outliers identified through principal component analyses (Supplementary Fig. 23). Post imputation, we
700 computed (unweighted) allelic correlations using a pruned set of SNPs, then filtered individuals so that no pair
701 remained with correlation greater than c , where $-c$ is the smallest observed pairwise correlation (c ranges from 0.029 to
702 0.038, depending on dataset). For our datasets, this filtering excluded relatively few individuals (on average 3.8%, with
703 maximum 11.6%). For all analyses, we include a minimum of 30 covariates: the top 20 eigenvectors from the allelic
704 correlation matrix just described, and projections onto the top 10 principal components computed from 1000 Genomes
705 samples.⁶⁰ For the 19 GWAS traits, we also include sex as a covariate, while for intraocular pressure and wide range
706 achievement test scores, we additionally include age. Supplementary Figure 24 reports the proportion of phenotypic
707 variance explained by each covariate. To check our filtering and covariate choices, we estimate the inflation of h_{SNP}^2 due
708 to population structure and residual relatedness³ (Supplementary Fig. 19). For the GWAS traits, we estimate that on

709 average h^2_{SNP} estimates are inflated by at most 3.1%, with the highest observed for ischaemic stroke (7.1%). For the 23
710 UCLEB traits, the average inflation is 0.3% (highest 2.3%).

711
712 **Single-SNP analysis:** Supplementary Figure 25 provides Manhattan Plots from logistic (case-control traits) and linear
713 regression (quantitative traits), performed using PLINK v.1.9. These analyses provide the summary statistics required
714 by LDSC. For the GWAS traits, we identified highly-associated SNPs ($P < 10^{-20}$) within the MHC for 6 of the GWAS
715 traits (rheumatoid arthritis, type 1 diabetes, psoriasis, ulcerative colitis, celiac disease and multiple sclerosis), while
716 rs2476601, a SNP within *PTPN22*, is highly associated with both rheumatoid arthritis and type 1 diabetes.^{61,62} For the
717 UCLEB traits, we find highly associated SNPs within *SCN10A* (PR Interval), *APOE* (total cholesterol, LDL cholesterol
718 and C-reactive protein) and *ZPR1* (triglyceride levels). For heritability analysis, these SNPs were pruned, then included
719 as additional fixed-effect covariates as described above.

720
721 **Computational requirements:** The most time-consuming aspect of analysis was genotype imputation; for a typically-
722 sized cohort (~3000 individuals) this took approximately one CPU-year (i.e., a few days on a 100-node cluster). Next is
723 computation of SNP weights, which for the GWAS traits (~4M SNPs) took approximately one CPU-month (again, this
724 can be near-perfectly parallelized). Finally, solving the mixed-model via REML would take between a few minutes for
725 the smaller traits (~5000 individuals) and a few hours for the largest (~14000 individuals). Memory-wise, the most
726 onerous task is solving the mixed-model, for which memory demands scale with n^2 ; however, even for the largest
727 dataset, this was less than 5Gb (when using multiple kinship matrices, LDAK allows for these to be read on-the-fly, so
728 that the memory demands are no higher than when using only one).

729
730

731 **Methods-only References**

732

- 733 43. Howie, B., Marchini, J. & Stephens, M. Genotype imputation with thousands of genomes. *G3* **1**, 457–470
734 (2011).
- 735 44. Hayes, B., Visscher, P. & Goddard, M. Increased accuracy of artificial selection by using the realized
736 relationship matrix. *Genet. Res.* **91**, 47–60 (2009).
- 737 45. Habier, D., Fernando, R. & Dekkers, J. The impact of genetic relationship information on genome-assisted
738 breeding values. *Genetics* **177**, 2389–2397 (2007).
- 739 46. Speed, D. & Balding, D. Relatedness in the post-genomic era: is it still useful? *Nat. Rev. Genet.* **16**, 33–44
740 (2014).
- 741 47. Hardy, G. Mendelian proportions in a mixed population. *Science (80)*. **28**, 49–50 (1908).
- 742 48. Weinberg, W. Über den Nachweis der Vererbung beim Menschen. *Jahreshefte des Vereins für Vaterländische*
743 *Naturkd. Württemb.* **64**, 368–382 (1908).
- 744 49. Lee, S. & van der Werf, J. An efficient variance component approach implementing an average information
745 REML suitable for combined LD and linkage mapping with a general complex pedigree. *Genet. Sel. Evol.* **38**,
746 25–43 (2006).
- 747 50. World Health Organization. Global tuberculosis report. (2014).
- 748 51. Gusev, A. *et al.* Quantifying Missing Heritability at Known GWAS Loci. *PLoS Genet.* **9**, e1003993 (2013).
- 749 52. Speed, D. & Balding, D. J. MultiBLUP: improved SNP-based prediction for complex traits. *Gen. Res.* **24**, 1550-
750 1557 (2014).
- 751 53. Zhou, X., Carbonetto, P. & Stephens, M. Polygenic modeling with Bayesian sparse linear mixed models. *PLoS*
752 *Genet.* **9**, e1003264 (2013).
- 753 54. Moser, G. *et al.* Simultaneous Discovery, Estimation and Prediction Analysis of Complex Traits Using a
754 Bayesian Mixture Model. *PLoS Genet.* **11**, e1004969 (2015).
- 755 55. Visscher, P. *et al.* Statistical Power to Detect Genetic (Co)Variance of Complex Traits Using SNP Data in
756 Unrelated Samples. *PLoS Genet.* e1004269 (2014).
- 757 56. Bhatia, G. *et al.* Haplotypes of common SNPs can explain missing heritability of complex diseases. (2016).
- 758 57. Tobin, M., Sheehan, N., Scurrah, K. & Burton, P. Adjusting for treatment effects in studies of quantitative traits:
759 antihypertensive therapy and systolic blood pressure. *Stat. Med.* **24**, 2911–2935 (2005).
- 760 58. Asselbergs, F. *et al.* Large-scale gene-centric meta-analysis across 32 studies identifies multiple lipid loci. *Am.*
761 *J. Hum. Genet.* **91**, 8230838 (2012).
- 762 59. Delaneau, O., Zagury, J. & Marchini, J. Improved whole-chromosome phasing for disease and population
763 genetic studies. *Nat. Methods* **10**, 5–6 (2013).
- 764 60. The 1000 Genomes Project Consortium. A map of human genome variation from population-scale sequencing.
765 *Nature* **467**, 1061–1073 (2010).
- 766 61. Todd, J. *et al.* Robust associations of four new chromosome regions from genome-wide analyses of type 1
767 diabetes. *Nat. Genet.* **39**, 857–864 (2007).
- 768 62. Plenge, R. *et al.* TRAF1-C5 as a risk locus for rheumatoid arthritis--a genomewide study. *N. Engl. J. Med.* **20**,
769 1199–1209 (2007).

770

771

772

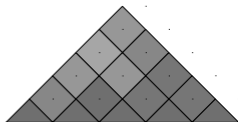
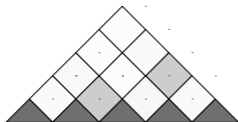
773

774

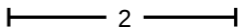
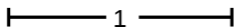
775

◇ Low Correlation

◆ High Correlation



Region



SNPs

X_1 X_2 X_3 X_4 X_5

X_6 X_7 X_8 X_9 X_{10}

Weights

1.0 0.8 0.8 1.0 1.0

1.0 0 0.9 0 0

Expected (relative) contribution to h_{SNP}^2 of each region:

GCTA Model

5

5

LDAC Model

4.6

1.9

